THE ASTROPHYSICAL JOURNAL, 501:616–623, 1998 July 10

DISCOVERY OF GAMMA-RAY EMISSION ABOVE 350 GeV FROM THE BL LACERTAE OBJECT 1ES 2344+514

M. CATANESE,[1] C. W. AKERLOF,[2] H. M. BADRAN,[3] S. D. BILLER,[4] I. H. BOND,[5] P. J. BOYLE,[6] S. M. BRADBURY,[5] J. H. BUCKLEY,[7] A. M. BURDETT,[5] J. BUSSÓNS GORDO,[6] D. A. CARTER-LEWIS,[1] M. F. CAWLEY,[8] V. CONNAUGHTON,[9] D. J. FEGAN,[6] J. P. FINLEY,[10] J. A. GAIDOS,[10] T. HALL,[10] A. M. HILLAS,[5] F. KRENNRICH,[1] R. C. LAMB,[11] R. W. LESSARD,[10] C. MASTERSON,[6] J. E. MCENERY,[6,12] G. MOHANTY,[1,13] J. QUINN,[12] A. J. RODGERS,[5] H. J. ROSE,[5] F. W. SAMUELSON,[1] M. S. SCHUBNELL,[2] G. H. SEMBROSKI,[10] R. SRINIVASAN,[10] T. C. WEEKES,[14] C. W. WILSON,[10] AND J. ZWEERINK[1]

Received 1997 December 4; accepted 1998 February 16

ABSTRACT

We present the discovery of gamma-ray emission greater than 350 GeV from the BL Lacertae (BL Lac) object 1ES 2344+514 with the Whipple Observatory 10 m gamma-ray telescope. This is the third BL Lac object detected at very high energies (VHE, $E > 300$ GeV), the other two being Markarian 421 (Mrk 421) and Mrk 501. These three active galactic nuclei are all X-ray selected and have the lowest known redshifts of any BL Lac objects currently identified with declination greater than 0°. The evidence for emission from 1ES 2344+514 comes mostly from an apparent flare on 1995 December 20 (UT) during which a 6 σ excess was detected with an average flux of $I(>350 \text{ GeV}) = 6.6 \pm 1.9 \times 10^{-11}$ photons cm^{-2} s^{-1}. This is approximately 63% of the VHE emission from the Crab Nebula, the standard candle in this field. Observations taken between 1995 October and 1996 January, excluding the night of the flare, yield a 4 σ detection indicating a flux level of $I(>350 \text{ GeV}) = 1.1 \pm 0.4 \times 10^{-11}$ photons cm^{-2} s^{-1}, or about 11% of the VHE Crab Nebula flux. Observations taken between 1996 September and 1997 January on this object did not yield a significant detection of a steady flux or any evidence of flaring activity. The 99.9% confidence level upper limit from these observations is $I(>350 \text{ GeV}) < 8.2 \times 10^{-12}$ photons cm^{-2} s^{-1}, $\lesssim$8% of the Crab Nebula flux. The low baseline emission level and variation in the nightly and yearly flux of 1ES 2344+514 are the same as the VHE emission characteristics of Mrk 421 and Mrk 501.

Subject headings: BL Lacertae objects: individual (1ES 2344+514) — gamma rays: observations

1. INTRODUCTION

The Whipple collaboration has discovered the two extragalactic sources of very high-energy (VHE, $E \gtrsim 300$ GeV) gamma rays, Markarian 421 (Punch et al. 1992) and Markarian 501 (Quinn et al. 1996). Both of these are BL Lacertae (BL Lac) objects, a subclass of the blazar class of active galactic nucleus (AGN). Blazars are the only class of AGN detected above 100 MeV by EGRET on the *Compton Gamma-Ray Observatory* (*CGRO*) (Fichtel et al. 1994; Thompson et al. 1995; Thompson et al. 1996), and BL Lac objects make up a significant fraction of the blazars detected by EGRET. The most striking feature of the VHE emission from Markarian (Mrk) 421 and Mrk 501 is the day scale or shorter flaring which has produced emission as high as 10 times the Crab flux (Gaidos et al. 1996), but flares on the order of $\frac{1}{2}$ the Crab flux are more typical (Buckley et al. 1996; Quinn et al. 1996; Quinn et al. 1997; McEnery et al. 1997). The baseline emission level for these two objects can be very low; Mrk 501 was initially detected to have a VHE flux 8% that of the Crab Nebula (Quinn et al. 1996), and Mrk 421 has dropped below the detection limit of the Whipple Observatory gamma-ray telescope for as long as a month (Buckley et al. 1996; McEnery et al. 1997).

Initial searches for extragalactic sources of VHE gamma rays by the Whipple collaboration concentrated mainly on blazars detected by EGRET or AGN of any type with small redshift (Kerrick et al. 1995). This approach led to the detection of Mrk 421, but only yielded upper limits for the other objects studied. Beginning in the spring of 1995, the Whipple collaboration initiated a more focused observation campaign on nearby BL Lac objects. The search list was mainly drawn from the work of Perlman et al. (1996), who identified 62 BL Lac objects from the Einstein Slew Survey sources (Elvis et al. 1992).[15] This list contained all of the prominent BL Lac objects (e.g., BL Lacertae, PKS

[1] Department of Physics and Astronomy, Iowa State University, Ames, IA 50011-3160.
[2] Randall Laboratory of Physics, University of Michigan, Ann Arbor, MI 48109-1120.
[3] Department of Physics, Faculty of Science, Tanta University, Tanta, Egypt.
[4] Department of Physics, Oxford University, Oxford, UK.
[5] Department of Physics, University of Leeds, Leeds, LS2 9JT, Yorkshire, England, UK.
[6] Experimental Physics Department, University College, Belfield, Dublin 4, Ireland.
[7] Department of Physics, Washington University, St. Louis, MO 63130.
[8] Physics Department, St. Patrick's College, Maynooth, County Kildare, Ireland.
[9] NASA, Marshall Space Flight Center, Huntsville, AL 35812.
[10] Department of Physics, Purdue University, West Lafayette, IN 47907.
[11] Space Radiation Laboratory, California Institute of Technology, Pasadena, CA 91125.
[12] Present address: Department of Physics, University of Utah, Salt Lake City, UT 84112.
[13] Present address: Laboratoire de Physique Nucléaire des Hautes Energies École Polytechnique, 91128 Palaiseau CEDEX, France.
[14] Fred Lawrence Whipple Observatory, Harvard-Smithsonian CfA, P.O. Box 97, Amado, AZ 85645-0097.

[15] We note that Mrk 501 was chosen as a candidate independently because of its similarities to Mrk 421.

2155−304, Mrk 421), but also significantly increased the number of BL Lac objects with known redshifts. In addition, because these objects were drawn from an X-ray survey, they were more likely to have emission spectra similar to Mrk 421 and Mrk 501. We limited the search to those sources with low redshifts (initially $z < 0.1$, but eventually extended to $z < 0.2$) in order to reduce the chances that the VHE emission would be significantly attenuated by interaction with the background intergalactic infrared radiation fields (Gould & Schréder 1967; Stecker, de Jager, & Salamon 1992). By the end of 1997, 18 of the Einstein Slew Survey BL Lac objects had been monitored with the Whipple Observatory telescope, including all 10 with $z < 0.1$ and declination greater than 0°. The first success of this observing program was the detection of Mrk 501 as a gamma-ray source. Since Mrk 501 was not identified in EGRET catalogs as a significant source, it highlighted the ability of ground-based gamma-ray telescopes to complement not only the results of the space-based gamma-ray telescopes but also to augment them. We report here on the second source detected in this BL Lac object search program, 1ES 2344+514.

1ES 2344+514 was only recently identified as a BL Lac object (Perlman et al. 1996), based on its lack of optical emission lines with observed equivalent width greater than 5 Å and its Ca II "break strength" being smaller than 25%. The latter criteria is indicative of the presence of a power-law continuum, and the former eliminates quasars. Perlman et al. (1996) determined this object to have a redshift of $z = 0.044$ based on absorption lines; it had no evident emission lines. This makes it the fourth closest known BL Lac object, after Mrk 421, Mrk 501, and EXO 0423.4−0840 (Padovani & Giommi 1995). Perlman et al. (1996) derive a 2 keV X-ray flux of 1.14 μJy, roughly one-third the flux detected for Mrk 421 and Mrk 501 in that same work, and measured an optical magnitude of $m_V = 15.5$ with no galaxy light subtraction. Measurements taken with the Very Large Array radio interferometer indicate that the BL Lac object 1ES 2344+514 radio emission is "pointlike," with more than 80% of its flux being from an unresolved point source (Patnaik et al. 1992; Perlman et al. 1996). The Green Bank radio survey lists its 5 GHz radio flux as 231 ± 25 mJy, which is about one-third and one-fourth the 5 GHz flux of Mrk 421 and Mrk 501, respectively.

In the following sections we outline the observation and analysis techniques (§ 2), detail the observations taken by the Whipple collaboration on 1ES 2344+514 between 1995 October and 1997 January (§ 3), and finally discuss the outcome and implications of those observations (§ 4).

2. OBSERVATION AND ANALYSIS TECHNIQUES

The VHE observations reported in this paper were made with the atmospheric Cerenkov imaging technique (Cawley & Weekes 1995; Reynolds et al. 1993) using the 10 m optical reflector located at the Whipple Observatory on Mount Hopkins in Arizona (elevation 2.3 km) (Cawley et al. 1990). A camera, consisting of photomultiplier tubes (PMTs) mounted in the focal plane of the reflector, records images of atmospheric Cerenkov radiation from air showers produced by gamma rays and cosmic rays. For most of the observations reported here, the camera consisted of 109 PMTs (each viewing a circular field of 0°.259 radius) with a total field of view (FOV) of 3°. In 1996 December, 42 additional PMTs were added to the camera, increasing the FOV to 3°.3. Because only a small fraction of the data presented here were taken with more than 109 PMTs, the analysis of this data only uses the original 109 PMTs. This makes the results consistent with the rest of the 1996/97 season and allows one set of parameter cuts to be used in the analysis. The telescope is sensitive to gamma rays with energies between approximately 200 GeV and 20 TeV.

We characterize each Cerenkov image using a moment analysis (Reynolds et al. 1993). The roughly elliptical shape of the image is described by the *length* and the *width* parameters, and its location and orientation within the telescope FOV are given by the *distance* and α parameters, respectively. We also determine the two highest signals recorded by the PMTs (max 1, max 2) and the amount of light in the image (size). The gamma-ray selection applied here utilizes the Supercuts95 criteria (Table 1; cf. Quinn et al. 1996; Catanese et al. 1996), which were optimized on contemporaneous Crab Nebula data to give the best sensitivity to point sources. Monte Carlo simulations indicate that this analysis results in an energy threshold of ∼350 GeV and an effective area of $\sim 3.5 \times 10^8$ cm^2. Details of the methods used to estimate the energy threshold and effective area are given elsewhere (Mohanty et al. 1998). The large effective area makes this technique very sensitive to short-term variability in sources.

2.1. *On/Off Observations*

The traditional mode of observing potential sources with the Whipple Observatory gamma-ray telescope and the method which is still usually used to confirm source signals and derive source spectra is the on/off mode of observation. In this type of observation, the putative source is tracked continuously for 28 minutes with the center of the telescope FOV positioned at the source location. In a 28 minute control, or "off," run the telescope tracks a position offset by 30 minutes in right ascension but with the same declination as the putative source. This off-source run begins exactly 30 sidereal minutes before or after the start of the on-source run so that the telescope tracks the same range of elevation and azimuth for both runs. Night sky brightness differences between the two observing fields are equalized off-line by software padding (Cawley et al. 1993). The significance of any excesses or deficits in the observations are calculated by using the maximum likelihood method of Li & Ma (1983).

This data collection technique has been shown to produce statistically stable gamma-ray count rates from the Crab Nebula over the course of several months (Quinn 1997) and to allow consistent, reproducible spectra to be derived for the existing sources (Mohanty et al. 1998; Hillas

TABLE 1

SUPERCUTS95

Gamma-Ray Range
max 1 > 100 d.c.[a]
max 2 > 80 d.c.
size > 400 d.c.
0°.16 < length < 0°.30
0°.073 < width < 0°.15
0°.51 < distance < 1°.10
α < 15°

[a] d.c. = digital counts. 1.0 d.c. ≈ 1.0 photoelectrons.

et al. 1998; Zweerink et al. 1997). However, this method requires excellent weather conditions to obtain consistent results between the on-source and the off-source runs so it reduces the observing time available. Also, because it only uses a small fraction of its gamma-ray–like events to estimate the background, it does not give the most statistically accurate background estimates possible.

2.2. *Tracking Observations*

For the reasons listed above, the more frequent mode of observation, particularly when searching for new sources, is the tracking mode. This mode of data collection for the Whipple Observatory gamma-ray telescope has been described previously (Kerrick et al. 1995; Quinn et al. 1996), but we do so again here for clarity and because some differences in the method of significance calculation are used. In this mode, only the on-source position is tracked, in runs of 28 minute duration, and no control observations are taken. To estimate the expected background, we use those events that pass all of the Supercuts95 criteria except orientation (characterized by the α parameter). We use events with values of α between 20° and 65° as the background region, as indicated in Figure 1. The lower bound gives a 5° buffer between the on-source region and the off-source region, to allow for some room for spillover events from the source region. The upper bound is chosen because the region beyond 65° is less stable from run to run and source to source because of the edge-of-field effects. As shown in the appendix, this nonstandard method of background estimation gives reliable results for a variety of observation fields. Using contemporaneous nonsource data, we find that the factor (called a tracking ratio) which converts the number of events in the region $\alpha = 20°–65°$ to an estimate of the on-source background ($\alpha = 0°–15°$) is $r = 0.292 \pm 0.004$ for the 1995/96 season and $r = 0.316 \pm 0.004$ for the 1996/97 season.

To convert the on-source and background counts to a significance S in the tracking analysis, we use a simple propagation of errors formula:

$$S = \frac{N_{\rm on} - r * N_{\rm bkd}}{\sqrt{N_{\rm on} + r^2 * N_{\rm bkd} + N_{\rm bkd}^2 * \Delta r^2}} , \quad (1)$$

where $N_{\rm on}$ is the number of events in the source region ($\alpha < 15°$), $N_{\rm bkd}$ is the number of events in the background region ($\alpha = 20°–65°$), and $r \pm \Delta r$ is the tracking ratio and its statistical uncertainty. The maximum likelihood method of

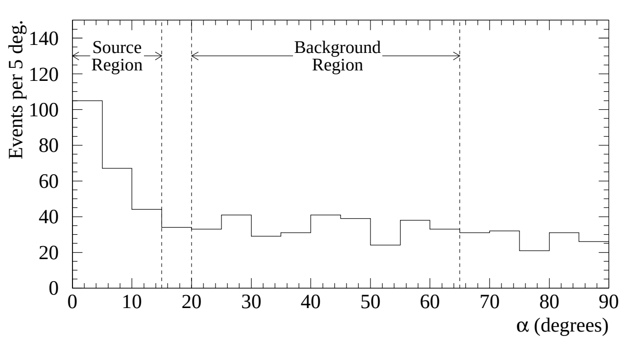

FIG. 1.—Distribution of α parameter values for events passing all but the α parameter cut of Supercuts95. These data were taken on the Crab Nebula between 1996 October and 1997 January. The source and background regions used in the tracking analysis described in the text are indicated.

Li & Ma (1983) cannot be used when the ratio for converting the background counts to a background estimate has any uncertainty. Li & Ma (1983) show that the estimate of the significance from equation (1) tends to be conservative when $r < 1$.

2.3. *Flux and Flux Upper Limit Estimation*

After Supercuts95 are applied to an on/off or tracking data set, we obtain a statistical significance as calculated with the methods described in § 2.1 and § 2.2, respectively, and a corresponding gamma-ray count rate in terms of counts per minute. If the excess is not statistically significant, we calculate a 99.9% confidence level (C.L.) upper limit on the count rate by using the method of Helene (1983). To convert these count rates or upper limits to fluxes, we first express them as a fraction of the Crab Nebula count rate for the same season. This corrects for season to season variations in factors like the PMT gain and mirror reflectivity which affect the telescope response, and therefore its gamma-ray count rate. For the 1995/96 season, the gamma-ray count rate for the Crab Nebula with a Supercuts95 analysis is 1.58 ± 0.05 per minute. In 1996/97, the Crab Nebula rate was 1.69 ± 0.07 per minute. Analysis of the Crab Nebula data shows that for runs taken under good weather conditions, the gamma-ray count rate does not change significantly within a season (Quinn 1997). So we can assume that the gamma-ray count rate for a source can be reliably compared to that of the Crab Nebula over the course of a season.

Once we have the flux or flux limit expressed as a fraction of the Crab Nebula count rate, we multiply it by the Crab Nebula flux (in units of photons $\rm cm^{-2}\ s^{-1}$) above the energy threshold of the observations. We determined the energy threshold for the observations reported here to be 350 GeV. The integral Crab Nebula photon flux is $I(>350\ {\rm GeV}) = (1.05 \pm 0.24) \times 10^{-10}$ photons $\rm cm^{-2}\ s^{-1}$ (Hillas et al. 1998). For flux estimates, we propagate the uncertainty in the Crab Nebula gamma-ray count rate and flux through to the final flux estimate, so the flux uncertainties have a significant contribution from the Crab Nebula flux uncertainty. The significance of an excess should thus not be estimated by the photon flux uncertainties. For the flux upper limits, we do not propagate through the Crab Nebula uncertainties. Upper limits are an estimate of the flux that could be present in the data set but not produce a significant excess. This is most accurately derived from the count rate because that is what determines the statistical significance of the excess. The Crab Nebula count rate and flux uncertainties affect only the normalization, so the flux upper limits quoted in terms of photons $\rm cm^{-2}\ s^{-1}$ have an uncertainty of $\sim$25%, mainly from the uncertainty in the Crab Nebula photon flux.

This flux calculation takes advantage of the fact that the VHE Crab Nebula flux is steady over at least a 7 yr period (Hillas et al. 1998) so that changes in the Crab Nebula count rate are most likely due to changes in the telescope sensitivity or threshold. The one disadvantage of this method is that it assumes that the spectrum of the putative source is similar to that of the Crab Nebula ($\propto E^{-2.5}$). Preliminary estimates of the spectrum for 1ES 2344+514 (to be presented in future work) indicate that it is not significantly different than this.

As shown below, 1ES 2344+514 is observed with an average elevation of $\sim$55°, much lower than the average

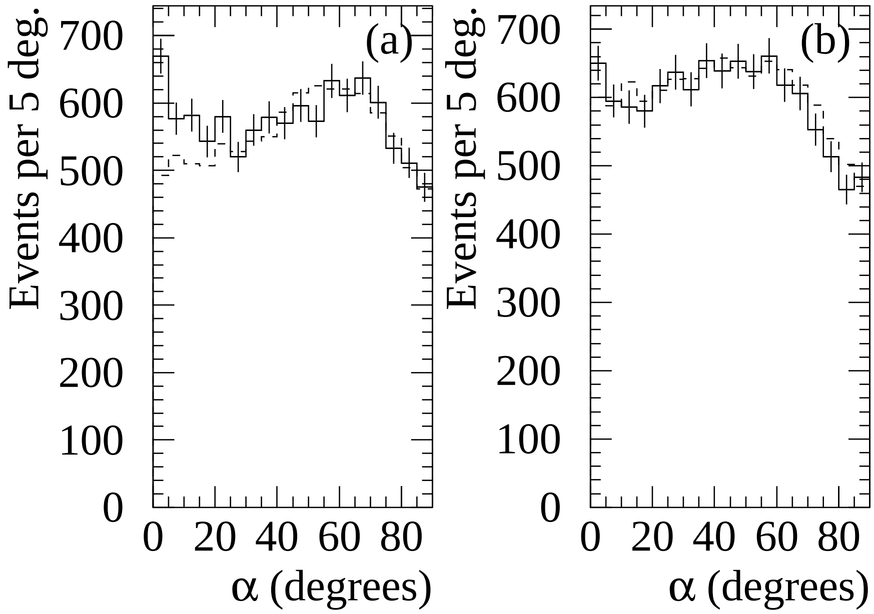

FIG. 2.—Distributions of the α parameter for 1ES 2344+514 for events that pass all other Supercuts95 cuts. Shown are all on-source data taken in (*a*) 1995/96 and (*b*) 1996/97. The dashed curves are the α distributions for the nonsource runs used in each season to estimate a tracking ratio (see text for details) normalized to the predicted background in the $\alpha = 0°$–$15°$ region.

elevation of the Crab Nebula observations ($\sim 72°$). While the telescope trigger rate does vary significantly with elevation, Supercuts95 analysis of the Crab Nebula indicates no significant variation in the gamma-ray count rate with elevation down to 50°. So, normalizing to the Crab Nebula count rate should be valid over that elevation range.

3. OBSERVATIONS AND RESULTS

For the 1995/96 observing season, 1ES 2344+514 was observed between October and January. After filtering the runs for bad weather and instrumental problems, the data set consists of 19 tracking runs (exposure = 9.0 hr) and 26 on/off pairs (exposure = 11.5 hr). The elevation of these runs varied from 37° to 70° with a mean of 55°. For the on/off pairs, using the Supercuts95 gamma-ray selection criteria, we obtain a significance of 2.9 σ with a corresponding excess count rate of 0.19 ± 0.07 per minute or a 99.9% C.L. upper limit of greater than 0.40 per minute. This converts to a flux upper limit of less than 0.25 times the VHE Crab Nebula flux rate or an integral flux upper limit of $I(>350$ GeV$) < 2.6 \times 10^{-11}$ photons cm^{-2} s^{-1}.

Combining all of the on-source runs, whether taken as on/off pairs or tracking runs, and using the tracking analysis described in § 2.2, we obtain a significance of 5.8 σ and a count rate of 0.25 ± 0.04 per minute. This translates into a flux of 0.16 ± 0.03 times the Crab Nebula flux or $I(>350$ GeV$) = 1.7 \pm 0.5 \times 10^{-11}$ photons cm^{-2} s^{-1}. The higher significance is due to a combination of having more data and the tracking analysis having a more statistically accurate estimate of the background. The count rates for the two data sets are consistent within statistical errors. These results are summarized in Table 2. Figure 2 shows the α distribution for the summed on-source runs, along with the α distribution for the nonsource runs used to estimate the tracking ratio. The latter distribution is normalized to the predicted background level from the tracking analysis.

For the 1996/97 observing season, 1ES 2344+514 was observed between September and January. After filtering for bad weather and instrumental problems, the data consist of 38 on/off pairs (exposure = 17.4 hr) and 16 tracking runs (exposure = 7.5 hr). The runs were taken at elevations ranging from 46° to 70° with an average elevation of 64°. For the on/off pairs, Supercuts95 analysis resulted in a -0.4 σ deficit with a corresponding 99.9% C.L. upper limit less than 0.15 counts per minute. This is equivalent to an upper limit on the flux of less than 0.09 times the Crab

TABLE 2

1ES 2344+514 OBSERVATION SUMMARY

Epoch	Data Type	Exposure (hr)	S (σ)	Rate[a] (counts per minute)	Flux[b] (Crab)	Flux[c] ($\times 10^{-11}$ cm^{-2} s^{-1})
1995/96	On/Off	11.5	2.9	<0.40	<0.25	<2.6
	Tracking[d]	20.5	5.8	0.25 ± 0.04	0.16 ± 0.03	1.7 ± 0.5
1995 Dec 20......	On/Off	1.38	4.2	0.87 ± 0.21	0.55 ± 0.13	5.8 ± 1.9
	Tracking	1.85	6.0	1.00 ± 0.17	0.63 ± 0.11	6.6 ± 1.9
1996/97	On/Off	17.4	-0.4	<0.15	<0.09	<0.93
	Tracking	24.9	0.4	<0.13	<0.08	<0.82

[a] The excess counts per minute, or the 99.9% C.L. upper limit on that quantity, passing Supercuts95.
[b] The flux, or 99.9% C.L. upper limit, is expressed as a fraction of the VHE Crab Nebula flux.
[c] The integral flux, or 99.9% C.L. upper limit, is quoted for $E > 350$ GeV.
[d] In this table, tracking refers to all on-source runs, including those taken as part of an on/off pair.

Nebula flux or $I(>350 \text{ GeV}) < 0.93 \times 10^{-11}$ photons $\text{cm}^{-2}\ \text{s}^{-1}$. For the combination of the on-source runs taken as part of the on/off pairs or as tracking runs, Supercuts95 analysis gives a 0.4 σ excess with a corresponding 99.9% C.L. upper limit less than 0.13 counts per minute. This upper limit is equivalent to less than 0.08 times the VHE Crab Nebula flux or $I(>350 \text{ GeV}) < 0.82 \times 10^{-11}$ photons $\text{cm}^{-2}\ \text{s}^{-1}$. These results are summarized in Table 2. The α parameter distribution for the tracking analysis is shown in Figure 2.

3.1. *Variability*

As discussed in § 1, both Mrk 421 and Mrk 501 exhibit low baseline levels of VHE emission, but with comparatively high-flux amplitude flares, typically lasting on the order of 1 day. So this sort of behavior should be expected in the VHE emission from other BL Lac objects if they emit VHE gamma rays. Therefore, we have searched for flaring activity from 1ES 2344+514 in both the 1995/96 and the 1996/97 observing seasons. The light curves showing the daily excess or deficit for all on-source data taken during the two seasons are shown in Figure 3. For 1996/97, the observations show no evidence of significant variability. The maximum daily excess has a significance of 1.8 σ, and the χ^2 probability that the excesses and deficits are consistent with statistical fluctuations about a common mean is 0.80. In contrast, for the 1995/96 season the χ^2 probability that the observations are consistent with constant emission is 3.5×10^{-8}. For comparison, the same analysis of the Crab Nebula data gives a χ^2 probability of constant emission of 0.78 in 1995/96 and 0.94 in 1996/97.

The most significant contribution to the variability in 1995/96 is 1995 December 20 (Fig. 3*a*, *arrow*). On that night, three on/off pairs and one tracking run were taken on 1ES 2344+514. The on/off pairs indicate a 4.2 σ excess and a flux of 0.55 ± 0.13 times the Crab Nebula flux, or $I(>350 \text{ GeV}) = (5.8 \pm 1.9) \times 10^{-11}$ photons $\text{cm}^{-2}\ \text{s}^{-1}$. A tracking analysis of all four on-source runs reveals a 6.0 σ excess with a corresponding flux of 0.63 ± 0.11 times the Crab Nebula flux, or $I(>350 \text{ GeV}) = (6.6 \pm 1.9) \times 10^{-11}$ photons cm^{-2} s^{-1}. The increase in significance for the tracking analysis is due to the additional run used. The fluxes for the on/off and tracking analyses are consistent within errors. The α parameter distribution for the night of the flare, clearly indicating the excess, is shown in Figure 4. There is no statistically significant variation in the flux within the night (see Fig. 5).

The flare on 1995 December 20 constitutes slightly over one-third of the excess gamma rays detected from 1ES 2344+514 in the 1995/96 season. When the data from that night are removed, the tracking analysis of all the remaining on-source runs reveals an excess of 4.0 σ and a corresponding flux of 0.11 ± 0.3 times the Crab Nebula flux, or $I(>350$

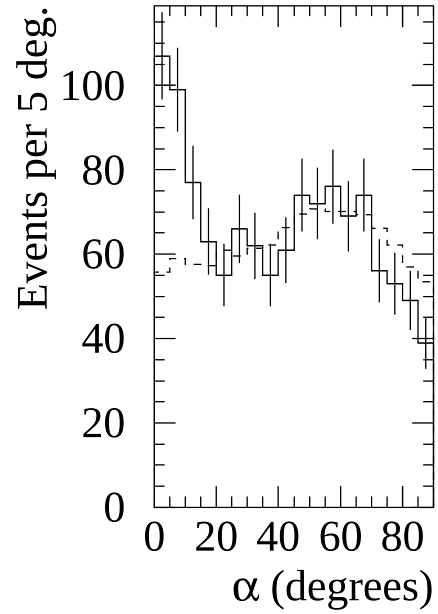

FIG. 4.—Distribution of the α parameter for all on-source data taken on 1ES 2344+514 on 1995 December 20 for events that pass all other Supercuts95 cuts. On/off data (*a*) and all on-source data (*b*) are shown. The dashed curve is the α distribution for the nonsource runs used to estimate the 1995/96 tracking ratio (see text for details) normalized to the predicted background in the $\alpha = 0°–15°$ region.

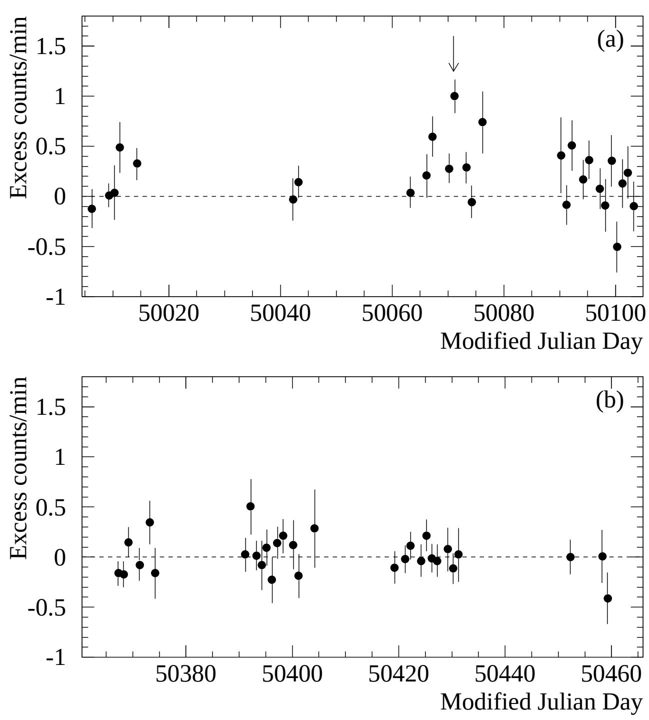

FIG. 3.—Light curves for all on-source data taken in (*a*) 1995/96 and (*b*) 1996/97 for 1ES 2344+514 passing Supercuts95. The uncertainties are 1 σ statistical errors. The arrow in (*a*) indicates the flare on 1995 December 20 (MJD 50071). In (*b*), MJD 50400 is 1996 November 13.

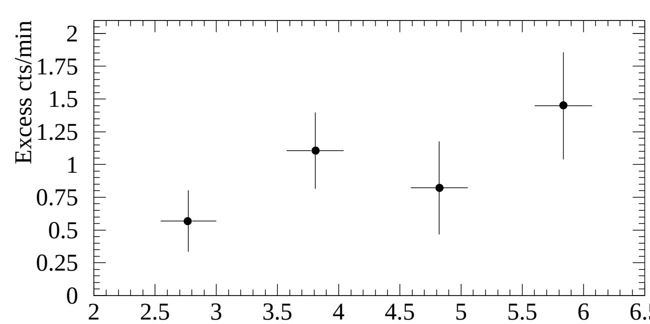

FIG. 5.—Light curve for all on-source observations of 1ES 2344+514 taken on 1995 December 20 for events passing Supercuts95. The error bars are 1 σ statistical uncertainties.

GeV) = $(1.1 \pm 0.4) \times 10^{-11}$ photons cm^{-2} s^{-1}. Thus, without the flare night, the evidence for emission from 1ES 2344+514 is marginal. The χ^2 probability that the emission is constant about the mean for the nonflare nights is 0.003, indicating evidence for further variability at the 3 σ level. From Figure 3 it is evident that any additional flaring was not significant on day scales. Given the low significance of the overall excess, further study of this possible variability is not feasible.

4. DISCUSSION

We have presented evidence of VHE emission from the BL Lac object 1ES 2344+514, as detected with the Whipple Observatory gamma-ray telescope. The emission is detectable only in 1995/96 and only with unambiguous statistical significance on 1995 December 20. On the latter date, the flux was ~60% that of the Crab Nebula. The baseline emission appeared to be ~10% of the Crab Nebula flux during 1995/96 and was less than 8% in 1996/97. This low emission level with a high-flux flare is what we would expect from a VHE-emitting BL Lac object, based on what has been observed of the VHE emission from the other known extragalactic VHE sources, Mrk 421 and Mrk 501. In fact, the initial detection of Mrk 501, as reported by Quinn et al. (1996), is almost completely analogous to the observations reported here for 1ES 2344+514. The initial detection of Mrk 501 indicated a mean flux equal to 8% that of the Crab Nebula, and in more than 66 hr of observations, only a single flare was detected with a flux equivalent to 50% of the Crab Nebula flux. The one difference is that in subsequent seasons Mrk 501 has become brighter (Quinn et al. 1997). If it had become dimmer, it would not have been detected in subsequent seasons, just as happened with 1ES 2344+514 in 1996/97.

The detection of 1ES 2344+514 is also consistent with Mrk 421 and Mrk 501 in that all three are nearby, X-ray–selected BL Lac objects (XBLs). By XBLs we mean here those BL Lac objects which have synchrotron spectra that extend into the UV to X-ray energy range. This extension makes them bright soft X-ray sources, hence the XBL label. The low redshift means the VHE emission will not be attenuated severely in the ~300 GeV energy range by interaction with background IR photons (Stecker, de Jager, & Salamon 1996; Biller et al. 1998). BL Lac objects have been suggested as better candidates for VHE emission than the flat-spectrum radio quasars (FSRQs) typically detected by EGRET because BL Lac objects lack broad emission lines in their optical spectra (Dermer & Schlickeiser 1994). The absence of such lines may indicate less VHE gamma-ray–absorbing material at the source. XBLs should be the best blazar candidates for VHE emission if the gamma rays are produced from inverse Compton scattering of low-energy photons by the same electrons that produce the synchrotron emission that dominates blazar spectra from radio to optical or X-ray wavelengths (e.g., Königl 1981; Maraschi et al. 1992; Bloom & Marscher 1996; Sikora, Begelman, & Rees 1994; Dermer, Schlickeiser, & Mastichiadis 1992). This is because the synchrotron spectrum of XBLs extends to higher energies than other blazars, like radio-selected BL Lac objects (RBLs) and FSRQs which have synchrotron cutoffs at optical wavelengths. This implies the presence of higher energy electrons in the jets of XBLs, so given similar magnetic fields and Doppler factors, XBLs should have an inverse Compton spectrum which extends to higher energies than those of RBLs or FSRQs (Sikora et al. 1994). This picture is consistent with the lack of VHE emission from nearby RBLs like BL Lacertae (Catanese et al. 1997a) and W Comae (Catanese et al. 1997b), which are EGRET sources (Catanese et al. 1997a; Thompson et al. 1996). However, it does not rule out models that produce gamma-ray emission as the product of extremely high-energy protons in the AGN jet (e.g., Mannheim 1993). More detections of BL Lac objects will be needed to investigate further that issue.

The spectral energy distribution (SED) of 1ES 2344+514 is indicated in Figure 6. Because the data are not contemporaneous, deriving limits on the jet parameters or making strong conclusions about the shape of the SED are not feasible. However, some general conclusions can be drawn. First, the SEDs of 1ES 2344+514, Mrk 421, and Mrk 501 are quite similar. Perlman et al. (1996) derive broadband spectral indices of $\alpha_{ox} = 1.18$, 1.14, and 1.15 and $\alpha_{ro} = 0.41$, 0.42, and 0.48 for 1ES 2344+514, Mrk 421, and Mrk 501, respectively. Interestingly, no other Slew Survey BL Lac object falls within these spectral index ranges, but because those data were not contemporaneous, this similarity could be coincidental. Second, 1ES 2344+514 is dimmer at every wavelength than Mrk 421 and Mrk 501; so it is perhaps not surprising that the VHE emission of 1ES 2344+514 appears to be weaker on average. If the X-ray power output were similar to that at 350 GeV, as it is in Mrk 421 (Macomb et al. 1995; Buckley et al. 1996), the gamma-ray flux detected in the flare would require an X-ray flux at 2 keV of 12 μJy, an increase of a factor of 10 over its detection flux. This is an extreme, but not unprecedented, increase in the X-ray flux. If the X-ray flux is higher than the gamma-ray flux, as it is with Mrk 501 (Catanese et al. 1997c), the

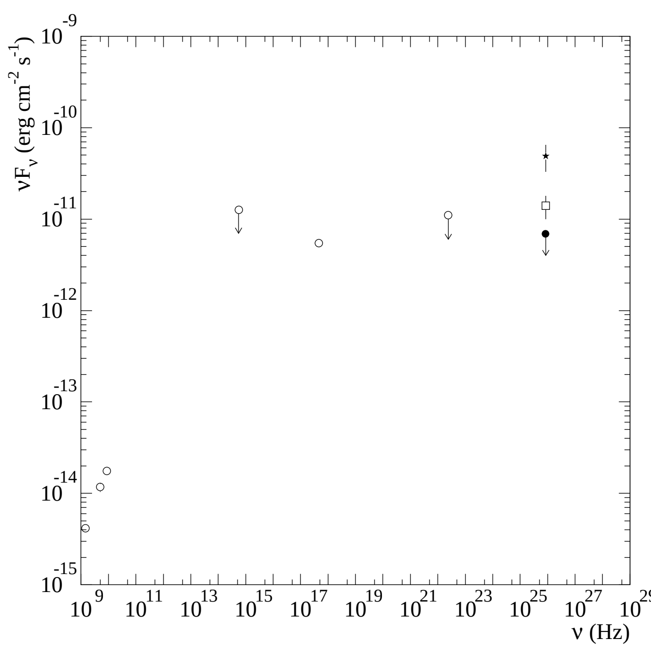

FIG. 6.—Spectral energy distribution of 1ES 2344+514. The VHE observations from 1995/96 (*open square*), 1996/97 (*filled circle*), and the flare flux of 1995 December 20 (*filled star*) are shown. Noncontemporaneous X-ray, optical, and radio fluxes are indicated by the open circles (Perlman et al. 1996; Patnaik et al. 1992; Gregory & Condon 1991). The optical flux is shown as an upper limit because the galaxy light contribution is not subtracted. In addition, the EGRET upper limit is shown (D. J. Thompson 1996, for the EGRET team, private communication).

X-ray flux requirements are even greater. Contemporaneous observations of 1ES 2344+514 will do much to clarify the shape of its SED for comparison with the other VHE-emitting BL Lac objects.

No other northern hemisphere imaging Cerenkov telescope has reported a detection or upper limit on 1ES 2344+514 at this time, though none were observing this object during 1995. Just as with Mrk 501, 1ES 2344+514 is not a source in the EGRET catalogs (Fichtel et al. 1994; Thompson et al. 1995; Thompson et al. 1996). The all-sky monitor on the *Rossi X-ray Timing Experiment* will allow better long-term multiwavelength monitoring of this object, and continued monitoring of this object with Cerenkov gamma-ray telescopes will hopefully confirm this object as a VHE gamma-ray source in the near future.

We acknowledge the technical assistance of K. Harris, T. Lappin, and E. Roache. We thank E. Perlman for providing an early version of his paper on the Einstein Slew Survey BL Lac objects which enabled us to pursue observations of 1ES 2344+514 in 1995. We also thank the EGRET team for providing the greater than 100 MeV flux upper limits for 1ES 2344+514. This research is supported by grants from the US Department of Energy and by NASA, by PPARC in the UK, and by Forbairt in Ireland.

APPENDIX

TRACKING MODE OBSERVATIONS

In the tracking observation mode, the on-source and background data are recorded at identical times, so changes in external weather conditions or system-wide variations in the electronics should affect both the on-source and the background regions similarly. The tracking mode also allows more on-source data to be taken in a given amount of time because no separate off-source run is needed. Finally, because more events (~ 3 times as many) are used in the background estimate than in the on/off analysis, it can lead to more statistically accurate estimates of the mean background level. However, the tracking analysis requires the distribution of background events versus α, the orientation parameter, to be the same from run to run in order to make accurate background estimates. Variations in the noise which do not affect the camera uniformly could change the α distribution. An example of such a variable noise source is the background light distribution due to stars within the FOV which changes with observation field and sky clarity. Also, a PMT which is turned off for a period of time, owing to a bright star or malfunction, affects the telescope response in a nonuniform way. If the α distribution changes, the factor that converts the background events (i.e., those with $\alpha = 20°–65°$) to an on-source ($\alpha = 0°–15°$) background estimate changes as well. If this factor, called a tracking ratio, varies for different observations, the tracking analysis is not a viable means of estimating the background.

To investigate these concerns, we have analyzed 148 hr of data taken on 20 nonsource observation fields in the 1995/96 season and 99 hr of data taken on 19 nonsource observation fields in the 1996/97 season. All runs were taken under good weather conditions. We analyzed these two data sets separately because they lead to different tracking ratios for the two seasons, as shown below. These observations consist of off-source and on-source runs for objects which do not reveal even a marginally significant signal. The only other selection made on these observation fields was that they did not have any stars within the FOV that produce a current greater than ~ 100 μA in more than one PMT. Stars which are that bright, such as ζ Tauri 1°.1 from the Crab Nebula, have a clear effect on the tracking ratio. The nonsource fields used here have a range of mean background brightness levels due to low-magnitude stars, and the elevations at which the observations were taken range from 20° to 85°. So no particularly restrictive constraints are placed on the data that we use to determine a tracking ratio. This is as it should be; if we must be very restrictive about the type of field we use in a tracking ratio estimate, then the tracking analysis loses its usefulness.

A tracking ratio of 0.292 ± 0.004 is found for the 1995/96 data set, and the 1996/97 data set indicates a tracking ratio of 0.316 ± 0.004. The differences in the two tracking ratios are most likely due to the fact that the telescope camera PMT gains were set to different values in the two seasons, resulting in a different response of the telescope to the Cerenkov and background light.

To determine whether the different observation fields show evidence of interrun, intersource, or intraseason variability in the tracking ratio, we applied several tests. To investigate the stability of the tracking ratio from run to run, we calculated the χ^2 probability that the tracking ratios for the individual runs were consistent with a single tracking ratio. For the 1995/96 data, the probability that the individual runs are drawn from the statistical distribution of a single tracking ratio is 0.23 and for the 1996/97 data it is 0.16. Both are thus consistent with arising from a single tracking ratio.

To test whether the different observation fields have different tracking ratios, we determined the significances of the excesses or deficits of the observations taken on the different fields and also calculated the χ^2 probability that the objects' mean tracking ratios were drawn from a distribution with a common mean. If the tracking ratio varies with observation field, using a single tracking ratio will result in a significant excess or deficit in some fields. Among the 39 fields used in the tracking ratios for the two seasons, only one had a statistical excess or deficit of more than 2 σ. This is expected 86% of the time given the number of trials in this test. The probability that the means of the tracking ratios are drawn from a single mean is 0.73 for the 1995/96 data and 0.44 for the 1996/97 season. So both tests indicate that the tracking ratios for the individual fields are consistent with a single tracking ratio.

The final test we applied was to see if the tracking ratio changed over the course of the season. To do this, we calculated the probability that the excess or deficit counts per minute for the summed objects were consistent with statistical fluctuations about a constant mean. If the tracking ratio changes with time, it should produce a consistent excess or deficit that gives a poor fit to the constant mean hypothesis. The χ^2 probability that the rate is constant is 0.68 for the 1995/96 data set and 0.25

for the 1996/97 season. Thus, we have no evidence that the tracking ratio changes significantly over the course of an observing season.

From these tests, we conclude that the single tracking ratio can be used for objects which do not have particularly bright stars within the telescope's FOV. We do, however, see a significant difference in the tracking ratio between seasons.

REFERENCES

Biller, S. D., et al. 1998, Phys. Rev. Lett., 80, 2992
Bloom, S. D., & Marscher, A. P. 1996, ApJ, 461, 657
Buckley, J. H., et al. 1996, ApJ, 472, L9
Catanese, M., et al. 1996, in Towards a Major Atmospheric Cherenkov Detector–IV (Padova, Italy), ed. M. Cresti, 335
———. 1997a, ApJ, 480, 562
———. 1997b, Proc. 25th Int. Cosmic Ray Conf. (Durban, South Africa), 3, 277
———. 1997c, ApJ, 487, L143
Cawley, M. F., et al. 1990, Exp. Astron., 1, 173
Cawley, M. F., et al. 1993, in Towards a Major Atmospheric Cherenkov Detector–II (Calgary, Canada), ed. R. C. Lamb, 176
Cawley, M. F., & Weekes, T. C. 1995, Exp. Astron., 6, 7
Dermer, C. D., & Schlickeiser, R. 1994, ApJS, 90, 945
Dermer, C. D., Schlickeiser, R., & Mastichiadis, A. 1992, A&A, 256, L27
Elvis, M., et al. 1992, ApJS, 80, 257
Fichtel, C. E., et al. 1994, ApJS, 94, 551
Gaidos, J. A., et al. 1996, Nature, 383, 319
Gould, J. R., & Schréder, G. P. 1967, Phys. Rev., 155, 1408
Gregory, P. C., & Condon, J. J. 1991, ApJS, 75, 1011
Helene, O. 1983, Nucl. Instrum. Methods Phys. Res., 212, 319
Hillas, A. M., et al. 1998, ApJ, submitted
Kerrick, A. D., et al. 1995, ApJ, 452, 588
Königl, A. 1981, ApJ, 243, 700
Li, T. P., & Ma, Y. Q. 1983, ApJ, 272, 317
Macomb, D. J., et al. 1995, ApJ, 449, L99
Mannheim, K. 1993, A&A, 269, 67
Maraschi, L., Ghisellini, G., & Celotti, A. 1992, ApJ, 397, L5
McEnery, J. E., et al. 1997, Proc. 25th Int. Cosmic Ray Conf. (Durban, South Africa), 3, 257
Mohanty, G., et al. 1998, Astropart. Phys., in press
Padovani, P., & Giommi, P. 1995, MNRAS, 277, 1477
Patnaik, A. R., Brown, I. W. A., Wilkinson, P. N., & Wrobel, J. M. 1992, MNRAS, 254, 655
Perlman, E.S., et al. 1996, ApJS, 104, 251
Punch, M., et al. 1992, Nature, 358, 477
Quinn, J. 1998, Ph.D. thesis, National Univ. Ireland
Quinn, J., et al. 1996, ApJ, 456, L83
———. 1997, Proc. 25th Int. Cosmic Ray Conf. (Durban, South Africa), 3, 249
Reynolds, P. T., et al. 1993, ApJ, 404, 206
Sikora, M., Begelman, M. C., & Rees, M. J. 1994, ApJ, 421, 153
Stecker, F. W., de Jager, O. C., & Salamon, M. 1992, ApJ, 390, L49
———. 1996, ApJ, 473, L75
Thompson, D. J., et al. 1995, ApJS, 101, 259
———. 1996, ApJS, 107, 227
Zweerink, J. A., et al. 1997, ApJ, 490, L141